AIAA JOURNAL
Vol. 40, No. 9, September 2002

Flow Control with Electrohydrodynamic Actuators

Guillermo Artana* and Juan D'Adamo†
University of Buenos Aires, 1063 Buenos Aires, Argentina
and
Luc Léger,‡ Eric Moreau,§ and Gérard Touchard¶
University of Poitiers, 86962 Futuroscope Cedex, France

The ability of an electrohydrodynamic actuator to modify the characteristics of a flow over a flat plate is analyzed. The device considered uses flush-mounted electrodes and a dc power supply to create a plasma sheet on the surface of the plate. We analyze the mechanism of formation of this plasma sheet, which has some similarities with the phenomenon of streamer formation. Experimental results are presented concerning flow visualizations obtained at low flow velocities (≈1 m/s) and velocity fields obtained with a particle image velocimetry technique for higher flow velocities (range 11.0–17.5 m/s). These results show that the discharge can induce an important acceleration of the flow close to the surface.

Introduction

CORONAS are self-sustaining discharges characterized by a strong inhomogeneity of the electric field configuration and electrodes having a low curvature radius. This configuration confines the ionization process to regions close to the high-field electrodes. Thus, in this phenomenon, there are active electrodes, surrounded by ionization regions where free charges are created, a low-field drift region where charged particles drift and react, and low-field passive electrodes. Coronas can be unipolar or bipolar if one or both electrodes are active electrodes. Bipolar coronas can lead to the formation of streamers, weakly conducting plasma filaments extending from one electrode and carrying their own ionization region ahead of themselves. Positive streamers are cathode directed and negative streamers anode directed.

The physics of corona discharge occurring in a gas close to an insulating surface has not been as widely studied as coronas without any extraneous bodies in the vicinity of the discharge.[1,2] Because the discharge involves the movement of ions as well as a large amount of neutral particles, this situation becomes of special interest in aerodynamics for flow and instabilities control.

The induced fluid motion is usually called electroconvection or sometimes electric wind. Coulombian electroconvection takes place if the coulombian forces acting on the fluid particles are predominant in relation to the polarization ones. This is usually the case when the fluid medium is air. The way the electric forces act on fluid particles may be explained by considering that ions in their drift motion from one electrode to the other will exchange momentum with the neutral fluid particles and induce their movement. Because currents involved in the process are so low that magnetic effects can be disregarded the phenomenon is described by the set of equations used in electrohydrodynamics (EHD) problems.

Received 1 May 2001; revision received 10 April 2002; accepted for publication 18 April 2002.

*Professor, Department of Mechanical Engineering, Faculty of Engineering, CONICET, Paseo Colón 850. Member AIAA.
†Ph.D. Student, Department of Mechanical Engineering, Faculty of Engineering.
‡Ph.D. Student, Laboratoire d'Etudes Aerodynamiques (Unité Mixte de Recherche 6609, Centre National de la Recherche Scientifique).
§Maitre de Conferences, Laboratoire d'Etudes Aerodynamiques (Unité Mixte de Recherche 6609, Centre National de la Recherche Scientifique).
¶Professor, Laboratoire d'Etudes Aerodynamiques (Unité Mixte de Recherche 6609, Centre National de la Recherche Scientifique).

In the present work, actuators based on electroconvection will be called EHD actuators. Main advantages of these actuators are that they have no moving part and a very short response time. (Delays are of the order of nanoseconds.) If the discharge takes place quite close to a surface, the velocity field close to this region can be greatly modified. Thus, in wall bounded or wake flows configurations, electroconvection is a good candidate to control the transition of boundary layers from laminar to turbulent types, to change the position of the separation line, or to modify the stability of coherent structures.

A large part of prior research of EHD actuators in air has been concerned with the possibility of heat transfer augmentation[3–7] and of drag reduction.[8–14] Also, some works have analyzed the effects of the electroconvection on the special flow configuration appearing in industrial process such as those in an electrostatic precipitator.[15–17] The effects of the ionization of the gas upstream of a shock wave and the possibility of using it to control the flow over hypersonic vehicles has also been receiving special attention.[18–21] Although previous research shows that injected ions can modify the characteristics and stability of the main flow, these devices (like most of the actuators currently considered in active fluid mechanic research) need substantial development. With a few exceptions,[10–12] most of the research has been undertaken with electrodes placed at some distance form the wall with an increase of momentum mainly in the direction normal to the surface.

If devices were developed with electrodes flush mounted on the surface, enabling the addition of momentum to the fluid tangentially to the wall, we think that it could be possible to achieve more effective control of some characteristics of the flows, such as the skin-friction forces, heat transfer, etc. On this principle, some EHD devices based on a surface-generated atmospheric rf plasma have been proposed. The one atmosphere uniform glow discharge (OAUGDP) device uses two electrodes separated by an insulating surface that avoids the knocking of the ions on the cathode. This prevents cathode heating and the formation of new avalanches or breakdown from electron secondary emission.[22] The authors claim that paraelectric forces associated to electric field gradients enable ion acceleration and, via particle collision, acceleration of the neutral particles. Other devices like the OAUGDP but with a polyphase rf power have been presented recently.[23,24]

The present work proposes a different approach because we use both electrodes flush mounted on an insulating surface and we consider a bipolar corona discharge obtained with a dc excitation. When this configuration is compared with an unipolar one, the electric field concentrates in a region closer to the insulating surface. In consequence, ions drift with trajectories lying on a region where fluid particles have low kinetic energy.

Recent results[25,26] indicate that, with this electrode configuration placed on insulating cylinders, some aspects of the discharge are

similar to the coronas' behavior. In Refs. 25 and 26, it is shown that under some circumstances a special regime can be observed: It is similar to a glow discharge as the drift region of the "normal" coronas almost fully disappears. From a technological point of view, the use of this configuration has advantages such as simplicity and, because of its uniformity, a high efficiency to transform electrical into mechanical power. However, to obtain a reliable device, it is still necessary to get better knowledge of the characteristic of the discharge under different conditions to operate it with a higher degree of control. The target of this work is to analyze the discharge characteristics produced by electrodes flush mounted on a surface of a flat plate and how the electroconvection they produce modifies the fluid mechanics occurring around the plate when traversed by an airflow.

Experimental Setup

In our study, the injection of ions is obtained with a dc corona discharge between a wire-type electrode (0.90-mm diam) and a plane electrode of aluminum foil (the same length as the wire). The electrodes are located flush mounted on the surface of a flat plate of poly methyl methacrylate (4 mm thick) as shown in Fig. 1. Two different high voltage sources of opposite polarity (+20 kV, −20 kV, 1.5 mA) impose a voltage difference between both electrodes.

The wire-type electrode is connected to the positive polarity source and the plate electrode to the negative one. When the voltage difference between both electrodes is increased, different discharge regimes can be established. The current measurement is undertaken with an electrometric circuit that can detect currents of 1 nA. The characteristic voltage current curves are determined using the setup shown in Fig. 2.

A plate, similar to that described but shorter, has been placed horizontally and parallel to the main flow in a wind tunnel (0–5 m/s, 0.28×0.28 m^2 rectangular cross section, turbulence level lower than 3%). The wire electrode was facing the flow in the frontal stagnation point. A schematic of the wind tunnel is shown in Fig. 3. Velocity measurements of the flow were taken with a micromanometer (accuracy 0.04 Pa) and a pitot probe.

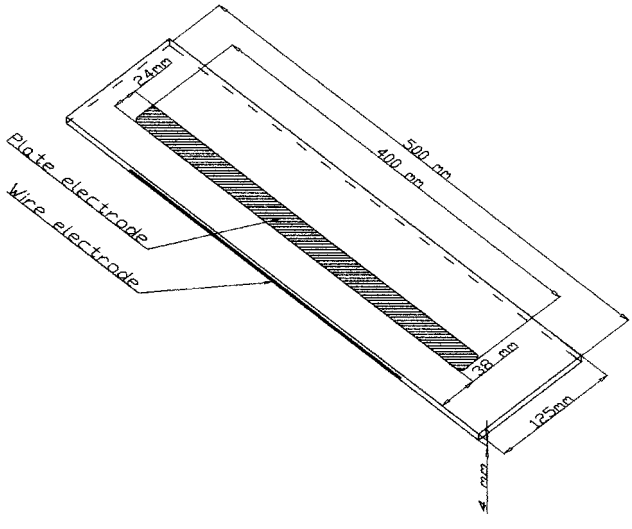

Fig. 1 Plate and electrode arrangement.

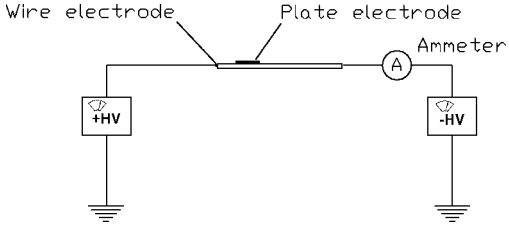

Fig. 2 Schematic of electric circuit.

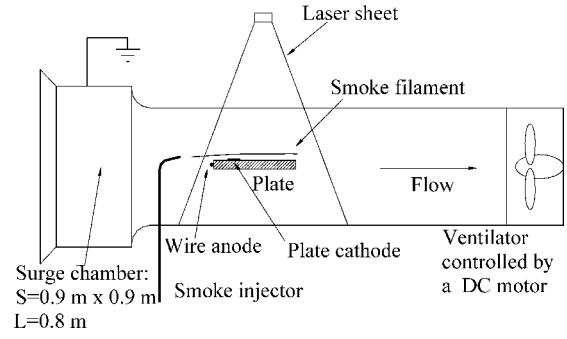

Fig. 3 Schematic of wind tunnel.

Visualizations at low velocities were done using a laser sheet produced by a 5-W argon-ion laser and a single smoke filament ($\phi = 2$ mm). Seeding was produced with an EI 514 Deltalab smoke generator that uses a pure cosmetic grade oil and that operated to obtain a cloud with a mean particle diameter of 0.3 μm. Images are recorded with a videocamera and then digitalized. Particle image velocimetry (PIV) measurements were done in a closed wind tunnel with a probe section of 0.50×0.50 m^2 and a range of velocities of 2–30 m/s. The experiments were conducted using the DANTEC system controlled by FlowMap® PIV. Interrogation area was 32×32 pixels with an overlap of 50%. Seeding was done with particles of a pure cosmetic grade oil, as in the visualization experiments, and with the same mean diameter. The system was illuminated with a laser sheet produced by a YAG laser of 200 mJ. In our experiments, each pulse had duration of 0.01 μs, and the time between a pair of pulses was 50 μs.

The progressive scan interline camera we used can produce images of 768×484 pixels. We considered 600 pairs of digital images taken every 0.1 s to obtain the velocity field of the airflow. The resolution for the distances of the field can be estimated as the product of the resolution of pixels (1/4 pixel) and a scale factor (1/14 mm/pixel). Then, the resolution of the velocity field can be estimated dividing the latter value by the time between a pair of pulses; in our case this leads to an uncertainty of $\Delta v = \frac{1}{4} \cdot \text{pixel}(1 \cdot \text{mm}/14 \cdot \text{pixel})(1/50\,\mu\text{s}) \cong 0.357$ m/s.

Experimental Results

Discharge Characteristics

The characteristics of the different discharge regimes in our case are described and a typical voltage–current curve is shown in Fig. 4. The different regimes are quite similar to the ones occurring in a cylindrical geometry with electrodes flush mounted as described in previous work.[25]

Spot-Type Regime

The discharge is concentrated in some visible spots of the wire, and by increasing the voltage difference, they can increase in number. Some of the spots may ionize in a plumelike type or may lead to a narrow channel quite attached to the surface. In Fig. 4, this regime corresponds to the range of currents lower than 0.2 mA/m

Generalized Glow Regime

At higher voltage differences, a regime characterized by a homogeneous luminescence can be observed. This luminescence occupies the whole interelectrode space almost all along the wire. The discharge makes the plate surface appear to be supporting a thin film of ionized air. This discharge is quite homogeneous noisy, and the current is quite stable with time. By visual inspection, it appears that the thickness of the ionized film is of the order of the thickness of the aluminum foil (50 μm). Measurements with a multiplier photometer indicate an intensity of the luminosity of the discharge close to 0.5 μ/m.

In Fig. 4, this regime corresponds to currents between 0.2 and 0.8 mA/m. The discharge is largely dependent on the quality of the finishing of the electrodes. Sometimes it is hard to start and can be promoted by blowing hot air toward the plate surface such as that produced with a hair drier. In the range of velocities of our

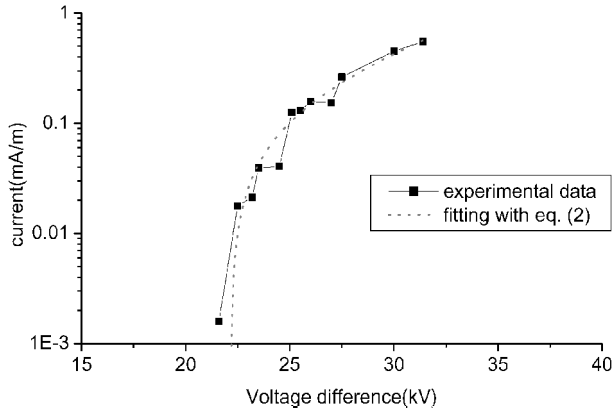

Fig. 4 Voltage current curve; electrode distance 38 mm and electrode length 400 mm.

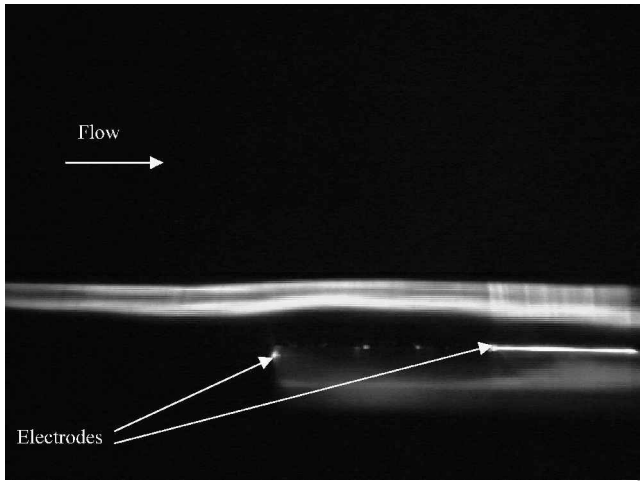

Fig. 5a Flow visualization; discharge off, $U_0 = 0.8$ m/s.

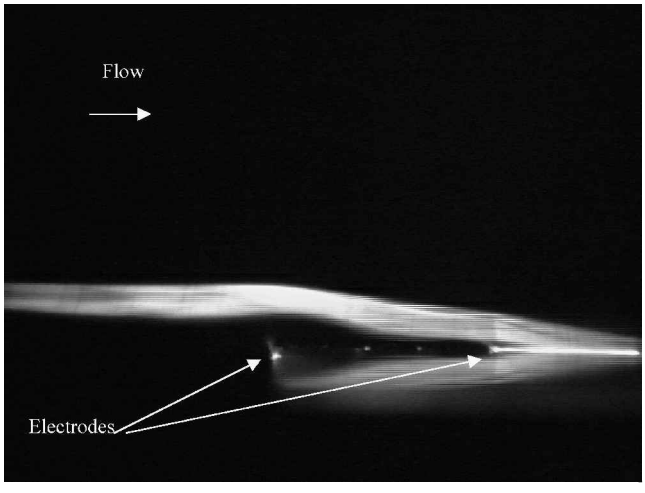

Fig. 5b Flow visualization; discharge on, $U_0 = 0.8$ m/s and $\Delta V = 33.0$ kV.

experiments, 0.5–20 m/s, the intensity of the current of the discharge was not significantly modified by a flow of air.

Filament-Type Regime

In this regime, some points of the wire have a concentrated discharge in an arborescent shape or in filament type. By the further increase of the voltage, some localized sparks appear following a nonrectilinear trajectory at a small distance from the surface.

In the present work we have undertaken the flow measurements in the generalized glow regime.

Flow Visualisation

Figures 5a and 5b are photographs showing typical visualizations at low velocity, $V \approx 1$ m/s. They show the changes on the smoke tracers filaments when the discharge is applied. (The wire electrode is upstream.)

PIV Data Processing

Each velocity field is filtered with a peak validation and a range validation filter. Peak validation filter is based on the detectability criterion,[27] which validates vectors with a ratio of the highest peak to the second highest peak in the correlation plane larger than a fixed value (1.2 in our case). The range validation filter enables the establishment of the range admitted for the modulus of the velocity vectors. In our case, we have considered a value of 2.0 times the flow velocity U_0 as the upper limit. When these filtering processes are used, about 50–100 vectors are removed from 1363 initial vectors.

An average on 600 vector fields is performed to obtain a mean velocity field of the airflow in one experiment. We show results corresponding to this mean velocity field in Figs. 6a–6c. Figures 6a–6c show the difference of these averaged vectors for the cases with discharge on and discharge off, at different flow velocities (11.0, 14.0, and 17.5 m/s).

Discussion

Physical Interpretation of the Electrical Results

In the past 20 years, different researchers[28–34] have been interested by a discharge in a configuration with some similarities with the one we consider here. Their goal was to obtain a uniform high current surface discharge at moderate voltages for gas lasers use. The device considered was similar to the one we used. It consisted of electrodes flush mounted on the surface of a dielectric plate, but they were excited with a pulsed voltage difference. Also a grounded electrode was placed in the reverse side of the plate.

The different discharge regimes for this pulsed discharge were described by Baranov et al.[31] and Lagarkov and Rutkevich.[34] They are quite similar to the ones we have observed with our dc excitation. They have also observed that, at a certain range of voltages and depending on specific conditions of the experiments, a uniform luminosity like a plasma sheet covering the space between both electrodes takes place. This phenomenon has been reported with different names such as sliding discharge, grazing discharge, or skimming discharge.

Rutkevich[33] and Lagarkov and Rutkevich[34] proposed a model of a stationary wave of ionization to describe the propagation of this discharge. They considered, as boundary conditions, a perfect dielectric solid with only polarization charges. Ion deposition and surface conduction were neglected. In this model the transverse component of the electric field near the dielectric surface plays an important role in the development of impact ionization. The nonuniformity of the impact ionization frequency in that direction is the main reason for forming the plasma sheet.

With this model, different parameters can be estimated (velocity of propagation, ion density, etc.), and an estimation of the thickness of the plasma sheet Δ is proposed as

$$\Delta = (1/\lambda_e)\,\ln(n_{ew}/n_0) \tag{1}$$

with λ_e the inverse of the thickness of the boundary layer for concentrations of electrons near the wall, n_{ew} the concentration of electrons in the gas immediately adjoining the wall, and n_0 a value that oscillates between 10^{12} and 10^{14} m^{-3}. Typical results of the plasma sheet obtained with this model oscillate between 0.1 and 1 mm, apparently of the same order as the one we observed.

The similarities that exists between both processes, the pulsed voltage case and the dc voltage case, indicate that the discharge with dc power should be a pulsating discharge because it occurs with the streamers produced with a point-to-plane electrode configuration. In our case the scheme could be a repetition of ionization waves. Each front of ionization screens the electric field and prevents a new process of ionization until its neutralization on the electrode.

The initiation of the plasma sheet by the use of hot air seems also to be associated, with the creation of lower density air channels[35]

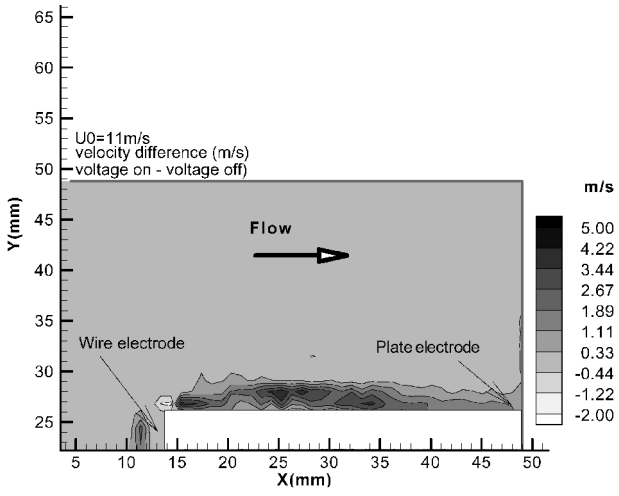

Fig. 6a Mean velocity field differences; $U_0 = 11.0$ m/s, discharge on with $\Delta V = 31.4$ kV.

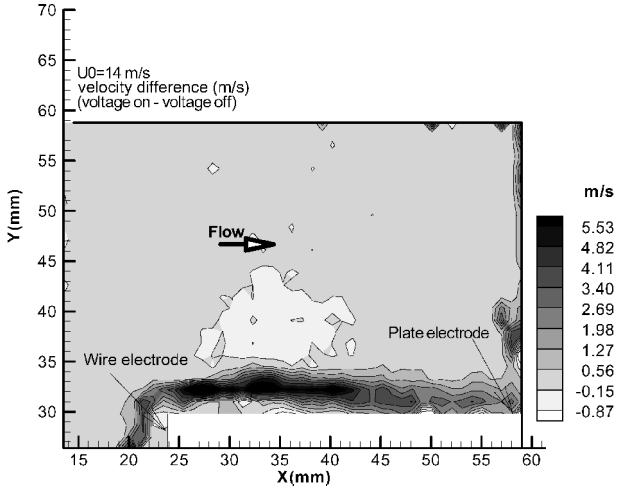

Fig. 6b Mean velocity field differences; $U_0 = 14.0$ m/s, discharge on with $\Delta V = 31.4$ kV.

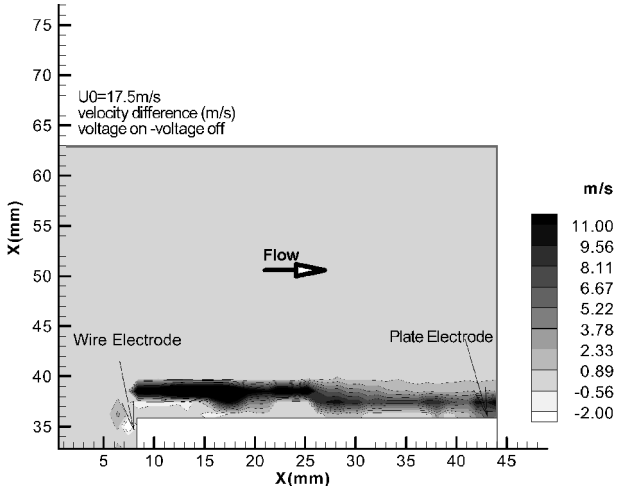

Fig. 6c Mean velocity field difference; $U_0 = 17.5$ m/s, discharge on with $\Delta V = 31.0$ kV.

as in point-to-plane repetitive streamers. This seems to be the more plausible mechanism to explain the formation of the plasma sheet with dc power, but further experiments and the use of a refined model including surface conduction and charge deposition–removal from the surface are still needed to describe fully the phenomenon. A rough analysis of the voltage–current curve can be undertaken if we use, as in other works,[10,11] the semi-empirical approach proposed by Seaver.[36] There, the voltage–current characteristics (in amperes per meter) are given by

$$I_c = (kT/\chi_i q R)\{\exp[\chi_i q(\Delta\phi - \phi_0)/kT] - 1\} \tag{2}$$

with I_c the current per unit length of electrode, $\Delta\phi$ the potential difference between the two electrodes, k the Boltzmann constant, T the absolute temperature, q the ion charge, χ_i a ratio known as the ion-to-neutral excess momentum concentration, and R a constant representing the gas-phase resistance outside the corona wire units (per meter ohms). Here ϕ_0 (in volts) is a constant associated with the voltage breakdown that can be estimated with

$$\phi_0 = E_c a \ln(S/a) \tag{3}$$

with E_c the corona onset voltage (in our case roughly $\approx 10^6$–10^7 V/m), S the electrode spacing, and a the curvature radius of the electrode. The fitting of our results with this function and least-square methods gives the following adjusted parameters: $\Phi_0 = 0.526$ kV, $R = 35.0$ kΩ/m, and $q\chi_i/kT = 0.148$ kV^{-1}. These values are similar to those obtained by El-Khabiry and Colver[10] and Colver and El-Khabiry[11] and the corresponding breakdown field in our case is $E_c = 2.7\,10^6$ V/m.

Finally, from our experiments, it can be observed that typical values of power consumption per unit area associated with the plasma sheet are about 500 W/m^2. They are of the same order than those needed to sustain a glow discharge with the OGADUP device.

Fluid Mechanics Result Interpretation

In flow visualization by smoke injection techniques or PIV experiments, the trajectories of the seeding particles and those of the surrounding fluid particles are usually considered to be the same. This occurs when the seeding particle follows closely the surrounding fluid particles. When there is a slipping velocity $V = U_p - U_f$ the trajectories may differ.

Although particle motion in a moving fluid is a rather complicated phenomena, Hinze's model (see Ref. 37) is usually accepted to describe (at least qualitatively) the motion of the seeding particles used in PIV experiments. The model gives an expression that enables the establishment of the limits of the particle size to track properly the flow. It expresses the following balance of forces:

$$\frac{\pi}{6} d_p^3 \rho_p \frac{\mathrm{d}\hat{U}_p}{\mathrm{d}t} = F_{\mathrm{st}} + F_p + F_f + F_u \tag{4}$$

where d_p is the diameter of the particle, U is velocity, ρ is density, subscript p refers to particle, and subscript f refers to fluid. Forces on the right-hand side of the equation are defined as

$$F_{\mathrm{st}} = -3\pi\mu d_p \hat{V}$$

$$F_p = \frac{\pi}{6} d_p^3 \rho_f \frac{\mathrm{d}\hat{U}_f}{\mathrm{d}t}$$

$$F_f = -\frac{\pi}{12} d_p^3 \rho_f \frac{\mathrm{d}\hat{V}}{\mathrm{d}t}$$

$$F_u = -\frac{3}{2} d_p^2 \sqrt{\pi\mu\rho_f} \int_{to}^{t} \frac{\mathrm{d}\hat{V}}{\mathrm{d}\zeta} \frac{\mathrm{d}\zeta}{\sqrt{t-\zeta}}$$

where μ is the coefficient of dynamic viscosity. F_{st} describes the viscous drag as given by Stokes law, F_p is the pressure gradient force, F_f takes into account the resistance of an inviscid fluid to acceleration of the seeding particle, and F_u is the Basset history integral that represents the drag force associated with unsteady motion.

The formula is valid under different assumptions (low particle density, particles are spherical, etc.) but one of the strongest assumptions in our case is that the electrostatic forces are negligible. Because some smoke particles can be charged by ion impact, coulombian forces would act on them affecting tracer trajectory. Thus, electrostatic forces should be added in our case to the left-hand side of the Hinze equation.

To evaluate the magnitude of the electrostatic forces we consider Bailey's work.[38] He indicates that when a particle is subjected to field-directed fluxes of positive and negative ions, both charging and neutralization processes occur simultaneously. Nevertheless, a

net charge develops, which depends on the difference in the rate at which the two flux types are intercepted. These rates are functions of the ion mobility and of the ionic density of each ion type. When a particle achieves a net charge level, the rate at which it receives charge of different signs is the same.

The maximum net charge level q_n that is attained after an exposure time of a few time constants is given by[38]

$$q_n = \pi d_p^2 \varepsilon_0 E_0 \left[\frac{2(\varepsilon_r - 1)}{\varepsilon_r + 2} + 1 \right] \frac{1 - (N_- \mu_- / N_+ \mu_+)^{\frac{1}{2}}}{1 + (N_- \mu_- / N_+ \mu_+)^{\frac{1}{2}}} \quad (5)$$

with ε_0 the Faraday constant, N_+ and N_- the density of positive and negative ions, and μ_+ and μ_- their respective mobilities. An upper limit of the attainable charge for droplets of nonpolar hydrocarbon (relative dielectric constant $\varepsilon_r \approx 2$) is obtained with

$$q_n \approx 1.5\pi d_p^2 \varepsilon_0 E_0 \quad (6)$$

When this limit and that coulombian forces F_c can be approximated with $F_c \approx E_0 \cdot q_n$ are considered, then F_c results to be proportional to the surface of the particle and to the square of the electric field E_0.

Because the influence of the electric forces is less important when the seeding particle diameter is very low, inspection of Eq. (4) corrected with the electrostatic forces shows that these last forces will be important only when the slipping velocity is very low. For instance, when a particle in air of $d_p = 1\ \mu$m and an electric field of $\approx 10^6$ V/m are considered, the ratio of the viscous to the electric forces is

$$F_{st}/F_{el} = -(3\pi \mu d_p / q_m \hat{E}_0)\hat{V} \approx 4.066(s/m)\hat{V} \quad (7)$$

where we see that the ratio is directly dependent on the slipping velocity V and that Stokes forces are much larger than electric ones except for low values of V.

In conclusion, for visualization and PIV analysis, the seeding particles should be chosen as large as possible to scatter most of the light. However, for reasons given earlier, the largest size is limited to particles of about 1 μm when a nonpolar hydrocarbon is the seeding material. When the data sheet given by the constructor of the smoke generator is considered, in our experiments the seeding particles we have used are in the range of 0.3 μm. Therefore, in our PIV and visualization experiments, the influence of coulombian forces on tracers trajectory in a first approach can be disregarded.

Flow Visualization

Flow visualization by smoke injection technique gives an idea of the changes in the flowfield that the discharge produces. In these experiments, we considered low flow velocities, $U_0 \approx 1$ m/s. Figure 5 shows results at 0.8 m/s flow velocities with the discharge operating in the generalized glow regime. We observe there that the filaments of the smoke tracers tend to approach to the plate when the discharge is applied. This indicates a tangential acceleration of the air close to the surface of the plate, creating a depression that tends to make the streamlines approach the surface. This intense effect is greatly reduced if the discharge operates in other regime (spot or filament type). There, the two-dimensional character of the flow is lost, and the coincidence of the discharge channels with the region of interest (the plane of visualization) is sometimes difficult.

PIV

We considered larger flow velocities in our PIV experiments. The results were obtained at flow velocities of 11.0–14.0 and 17.5 m/s and though corresponding to a very different range from those of flow visualization they are in good agreement. We observe in Figs. 6a–6c a relatively important acceleration of the fluid close to the plate surface when compared to the flow velocity. Comparison of Figs. 6a–6c shows that the velocity differences produced by the EHD actuator in the region close to the wall are more important as flow velocities increase. The maximum values of the differences detected are 4.6, 4.9, and 10.7 m/s, corresponding to flow velocities of 11.0, 14.0, and 17.5 m/s, respectively. This indicates that in the range of velocities where PIV has been done the electric forces and

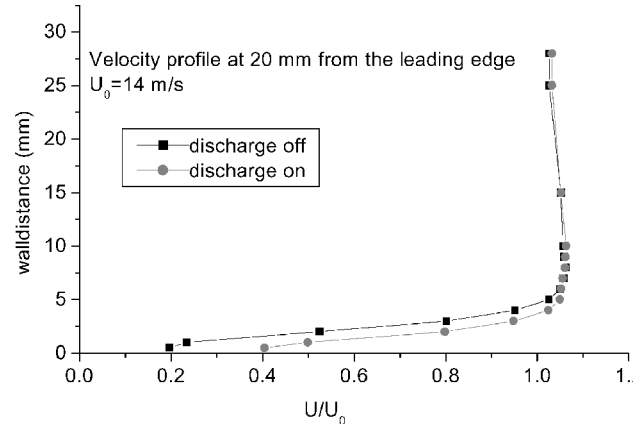

Fig. 7 Typical velocity profile ratio: streamwise station 20 mm from the leading edge, U_0 = 14.0 m/s, discharge voltage ΔV = 31.0 kV.

the conversion of electrical to mechanical power increase with flow velocity.

Our results indicate that in the fluid and ion flow configuration adopted, the interaction of ions with neutral fluid particles in the region close to the wall seems to depend on the main stream velocity. This effect, in consequence, is dependent on the flowfield close to the wall and is larger when the fluid particles outside the region where viscous forces are important are animated with more important velocities. The effects of the actuator on the boundary condition of the flow produce the modifications of the flowfield observed. However, these effects in principle should not be reduced to only a momentum adding to the boundary layer.

The ionization of the fluid also produces changes on its physical properties (density, viscosity, etc.) in regions of the flow close to the wall. Then, a model that includes these changes as well as the momentum added to the flow in the boundary layer should be proposed. With our experiments, we cannot distinguish the relative importance of each effect. A numerical model approach and further experiments could give some insight to this problem.

Figure 7 shows the shape of the velocity profiles ratios obtained with the discharge on and off. Figures 8 show the difference of these velocities ratio profiles at different streamwise stations and for different flow velocities. We can observe in Figs. 7 and 8 how the electric forces modify the velocity profile in the field of view of our experiments. The magnitude of the velocity differences with discharge on and off are larger in a region about 1.5 cm measured from the plate surface. This region becomes more important with increasing distances from the leading edge.

We observe in Figs. 8a–8c that the changes in the velocity field produced by the EHD actuator are more pronounced in fluid layers close to the wall. At larger distances from the leading edge, the changes tend to be more uniform, and velocities differences can be detected in layers at larger wall distances. This can be explained considering that the momentum changes on the boundary layers produce changes on the flow that are subjected simultaneously to diffusion (mainly in the direction normal to the surface) and convection processes (mainly in the flow direction).

At positions close to the leading edge, streamlines far from the surface "feel" less what happens at the boundary than those quite close to it. As we consider positions at larger distances from the leading edges, diffusion modifies the momentum of the less perturbed layers (those far from the surface) and the velocity profile modifications penetrate more in the fluid. The shapes of curves of Fig. 7 are similar to those obtained with the OGADUP with pitot probes placed downstream of the device.[22]

Comparing EHD with OGADUP, we observe that in both cases an important acceleration has been detected. However, the acceleration of the fluid layers close to the surface produced with the EHD actuator does not have the nonuniformities in the spanwise directions shown in Ref. 22. Also, our results show larger changes produced with the EHD device than those with the OGADUP. However, a direct comparison of the performance of both actuators is not possible

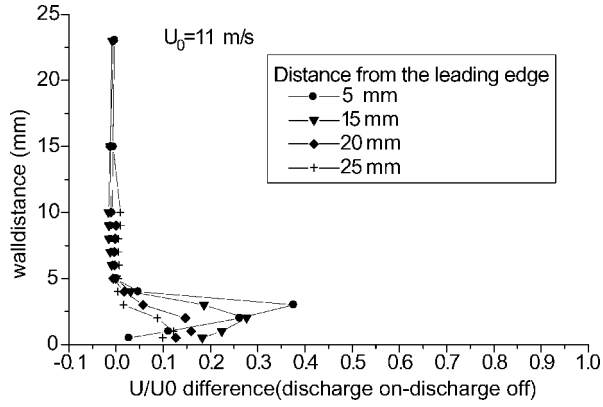

Fig. 8a Velocity difference ratio profiles at different streamwise stations; U_0 = 11.0 m/s, discharge voltage ΔV = 31.4 kV.

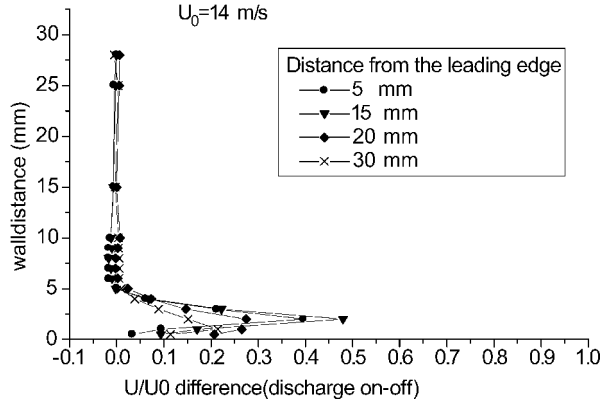

Fig. 8b Velocity difference ratio profiles at different streamwise stations; U_0 = 14.0 m/s, discharge voltage ΔV = 31.4 kV.

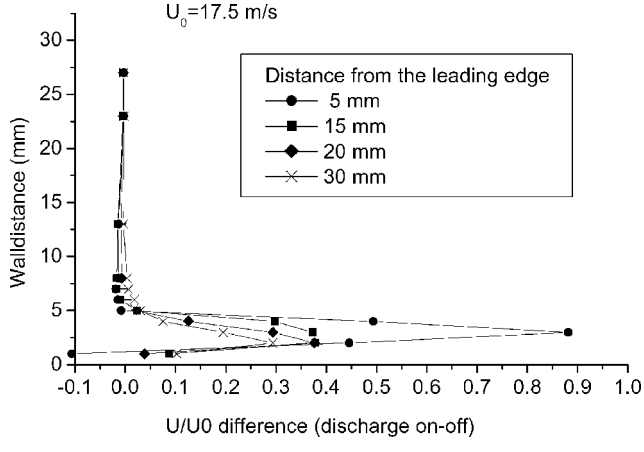

Fig. 8c Velocity difference profiles at different streamwise stations; U_0 = 17.5 m/s, discharge voltage ΔV = 31.0 kV.

because the values obtained correspond to different streamwise locations.

Conclusions

We show that the characteristics of a corona discharge in the proximity of extraneous bodies are quite similar if this body has a cylindrical geometry or if it is of the flat plate type. The physical phenomena involved in the description of the plasma sheet creation are similar to the ones occurring in the formation of repetitive ionization waves, like the ones appearing in streamers. The effect of the dc corona discharge on the flow operating in the generalized glow regime is very distinctive because of two main factors: 1) its intensity (luminescence in all of the arc distance could be associated to ionization produced by high-velocity charged particles) and 2) the homogeneity of the discharge occurring all along the electrode length. From flow visualization results, it can be concluded that at low Reynolds number the effect of the discharge in the fluid dynamics close to the wall is important. However, this effect is highly dependent on the regime of discharge considered.

PIV measurements enabled us to corroborate this and to conclude that strong effects of this kind of EHD actuators on the flow are not limited to very small flow velocities as suggested by Roth and Sherman.[22] The EHD actuator adds momentum in the boundary layer but also may change the fluid properties in regions close to the wall. These uniform changes in the boundary condition produce an effect on the flow that seem to be more important at larger flow velocities.

In consequence, our results indicate that, in the range of velocities considered, an important effect on the control of heat transfer or in drag reduction may be expected to be attained with this actuator. Experiments considering a larger range of flow velocities and an optimization of the electrode configuration should be considered in a future work.

Acknowledgments

This research has been supported with Grants UBACYT AI-25 and PICT 12-02177 of the Argentine government. We would like to thank the authorities of the University of Poitiers for inviting G. Artana to the Laboratorie d'Etudes Aerodynamiques during January and February of 2000, where particle image velocimetry and visualization experiments were done.

References

[1]Loeb, L., *Electrical Coronas*, Univ. of California Press, Berkeley, CA, 1965, pp. 552–608.

[2]Goldman, M., and Sigmond, R., "Corona and Insulation," *IEEE Transactions on Electrical Insulation*, Vol. 17, No. 2, 1982, pp. 90–105.

[3]Velkoff, H., and Godfrey, R., "Low Velocity Heat Transfer to a Plate in the Presence of a Corona Discharge in Air," *Journal of Heat Transfer*, Vol. 101, Feb. 1979, pp. 157–163.

[4]Velkoff, H., Kulacki, F., "Electrostatic Cooling," American Society of Mechanical Engineers, ASME Paper 77-DE-36, 1977.

[5]Kibler, K., and Carter, G., "Electrocooling in Gases," *Journal of Applied Physics*, Vol. 45, 1974, pp. 4436–4439.

[6]Ohadi, M., Li, S., and Dessiatoun, S., "Electrostatic Heat Transfer Enhancement in a Tube Bundle Gas-to-Gas Heat Exchanger," *Journal of Enhanced Heat Transfer*, Vol. 1, 1994, pp. 327–335.

[7]Ohadi, M., Nelson, D., and Zia, S., "Heat Transfer Enhancement of Laminar and Turbulent Pipe Flow via Corona Discharge," *International Journal of Heat and Mass Transfer*, Vol. 34, No. 4, 1991, pp. 1175–1187.

[8]Noger, C., Chang, J. S., and Touchard, G., "Active Controls of Electrohydrodynamically Induced Secondary Flow in Corona Discharge Reactor," *Proceedings of the 2nd International Symposium on Non-Thermal Plasma Technology and Pollution Control*, edited by J. Chang, 1997, pp. 136–141.

[9]Vilela Mendes, R., and Dente, J., "Boundary Layer Control by Electric Fields," *Journal of Fluids Engineering*, Vol. 120, No. 3, 1998, pp. 626–629.

[10]El-Khabiry, S., and Colver, G., "Drag Reduction by D. C. Corona Discharge Along an Electrically Conductive Flat Plate for Small Reynolds Number Flows," *Physics of Fluids*, Vol. 9, No. 3, 1997, pp. 587–599.

[11]Colver, G., and El-Khabiry, S., "Modeling of DC Corona Discharge Along an Electrically Conductive Flat Plate with Gas Flow," *IEEE Transactions on Industry Applications*, Vol. 35, No. 2, 1999, pp. 387–394.

[12]Soetomo, F., "The Influence of High Voltage Discharge on Flat Plate Drag at Low Reynolds Number Air Flow," M.S. Thesis, Dept. of Mechanical Engineering, Iowa State Univ., Ames, IA, Sept. 1992.

[13]Bushnell, D., "Turbulent Drag Reduction for External Flows," AIAA Paper 83-0227, Jan. 1983.

[14]Malik, M., Weinstein, L., and Hussaini, M., "Ion Wind Drag Reduction," AIAA Paper 83-0231, Jan. 1983.

[15]Kallio, G., and Stock, D., "Interaction of Electrostatics and Fluid Dynamic Fields in Wire-Plate Electrostatic Precipitators," *Journal of Fluid Mechanics*, Vol. 249, 1992, pp. 133–166.

[16]Soldati, A., "Turbulence Control and Drag Reduction by Means of Large-scale Electrohydrodinamic Structures," *Proceedings of the International Workshop on Electrical Conduction, Convection, and Breakdown in Fluids*, edited by P. Atten and A. Denat, Grenoble, France, 1998, pp. 119–125.

[17]Soldati, A., and Banerjee, S., "Turbulence Modification by Organized Electrohydrodynamic Flows," *Physics of Fluids*, Vol. 10, No. 7, 1998, pp. 1742–1756.

[18]Cahn, M., and Andrew, G., "Electroaerodynamics in Supersonic Flow," AIAA Paper 68-24, Jan. 1968.

[19]Cheng, S., and Goldburg, A., "Analysis of the Possibility of Reduction of Sonic Boom by Electroaerodynamic Devices," AIAA Paper 69-38, Jan. 1969.

[20]Poggie, J., "Modeling the Propagation of a Shock Wave Through a Glow Discharge," *AIAA Journal*, Vol. 38, No. 8, 2000, pp. 1411–1418.

[21]Adamovich, I., Subramanian, V., Rich, J., and Macheret, S., "Phenomenological Analysis of Shock-Wave Propagation in Weakly Ionized Plasmas," *AIAA Journal*, Vol. 36, No. 5, 1998, pp. 816–822.

[22]Roth, J. R., and Sherman, D., "Boundary Layer Flow Control with a One Atmosphere Uniform Glow Discharge Surface Plasma," AIAA Paper 98-0328, Jan. 1998.

[23]Corke, T., and Mattalis, E., "Phased Plasma Arrays for Unsteady Flow Control," AIAA Paper 2000-2323, June 2000.

[24]Lorber, P., McCormick, D., Pollack, M., Breuer, K., Corke, T., and Anderson, I., "Rotorcraft Retreating Blade Stall Control," AIAA Paper 2000-2475, June 2000.

[25]Artana, G., Desimone, G., and Touchard, G., "Study of the Changes in the Flow Around a Cylinder Caused by Electroconvection," *Electrostatics'99*, IOP Publ., Ltd, Bristol, England, U.K., 1999, pp. 147–152.

[26]Desimone, G., DiPrimio, G., and Artana, G., "Modification of the Flow Around a Cylinder by Means of Electrodes Placed on its Surface," *Colloque de la Societé Francaise d'Electrostatique*, LEA, Poitiers, France, 1999, pp. 80–84.

[27]Keane, R., and Adrian, R., "Theory of Cross Correlation Analysis of PIV Images," *Applied Scientific Research*, Vol. 49, No. 3, 1992, pp. 191–215.

[28]Andreev, S., Belousova, I., Dashuk, P., Zaroslov, D., Zobov, E., Karlov, N., Kuz'min, G., Nikiforov, S., and Prokhorov, A., "Plasma-Sheet Co_2 Laser," *Soviet Journal of Quantum Electronics*, Vol. 6, No. 8, 1976, pp. 931–934.

[29]Dashuk, P., and Kulakov, S., "Formation of an Electron Beam in the Plasma of a Skimming Discharge," *Soviet Technical Physics Letters*, Vol. 7, No. 11, 1981, pp. 563–565.

[30]Atanasov, P., and Grozdanov, K., "Simultaneous Ultraviolet and Infrared Emission in a Sliding-Discharge Excited Laser," *IEEE Journal of Quantum Electronics*, Vol. 32, No. 7, 1996, pp. 1122–1125.

[31]Baranov, V., Borisov, V., Vysikailo, F., Kiryukhin, B., and Khristoforov, O., "Analysis of Sliding Discharge Formation," Kurchatov Inst. of Atomic Energy, Rept. 3472/7, Moscow, 1981 (in Russian).

[32]Beverly, R., "Electrical Gasdynamics and Radiative Properties of Planar Surface Discharge," *Journal of Applied Physics*, Vol. 60, No. 1, 1986, pp. 104–124.

[33]Rutkevich, I., "Structure of a Grazing Discharge Front," *Soviet Physics—Technical Physics*, Vol. 31, No. 7, 1986, pp. 841–842.

[34]Lagarkov, A., and Rutkevich, I., *Ioniztion Waves in Electrical Breakdown of Gases*, Springer-Verlag, New York, 1993, pp. 195–207.

[35]Sigmond, R., and Goldman, M., "Positive Streamer Propagation in Short Gaps in Ambient Air," *Proceedings of the 15th International Conference on Phenomena in Ionized Gases*, IUPAP, Minsk, 1981, pp. 649–651.

[36]Seaver, A., "Onset Potential for Unipolar Charge Injection," *Proceedings of the Annual Meeting of the IEEE Industry Applications Society*, 1993, pp. 1–7.

[37]Fuchs, N., *The Mechanics of Aerosols*, Dover, New York, 1964, pp. 21–180.

[38]Bailey, A., *Electrostatic Spraying of Liquids*, Wiley, New York, 1988, pp. 38–41.

J. P. Gore
Associate Editor